Journal of Ceramic Processing Research. Vol. 6, No. 3, pp. 230~235 (2005)

J O U R N A L O F
Ceramic Processing Research

Calcium aluminate composites with controlled duplex structures: II. Microstructural development and mechanical properties*

H.J. Liaw and Wen-Cheng. J. Wei*
Institute of Materials Science and Engineering, National Taiwan University, Taipei, Taiwan 106, ROC

This study used monocalcium aluminate ($CaAl_2O_4$, CA) to produce ceramic composites with duplex microstructures by hydration and gelation reactions of the aluminate, and compared the properties with those made by a die-pressing process with mixed powders. The microstructure of sintered bodies, the fracture strengths and toughness of the composites with and without thermal shock was characterized by different techniques. Experimental results show that the composites with the addition of CA resulted in the formation of CA_6 ($CaO*6Al_2O_3$) platelets, so as to reveal two types of microstructures, either in a cluster of agglomerated platelets or with a uniform distribution of platelet CA_6 grains. The former, which appeared as a duplex microstructure consisted of a dense matrix and distributed clusters of CA_6 platelets, gave an improvement in toughness and thermal shock resistance. The toughness mechanisms of the samples with duplex microstructures are discussed.

Key words: calcium aluminate, composite, platelets, duplex, microstructure.

Introduction

CaO segregation at the grain boundaries of Al_2O_3 grains has been characterized and reported for decades [1]. Even 30 ppm of Ca impurity induces abnormal grain growth after sintering at 1900 °C for 1 h [2]. The driving force for the segregation was dominated by the misfit strain of the Ca ions in the alumina lattice. The CaO has also been treated as a liquid-phase former which is responsible for the formation of abnormal Al_2O_3 grain growth [3].

Calcium aluminates, for instance CA, $C_{12}A_7$, and C_3A, where C stands for CaO and A for Al_2O_3, were used in a previous report to prepare CaO-Al_2O_3 composites [4]. Among the aluminates, CA powder is the important ingredient used for the hydration and gelation of the alumina in an aqueous state The CA confines one eutectic composition with the $C_{12}A_7$ phase at the temperature of 1360 °C in the Al_2O_3-CaO system. Liquid phase formation at temperatures greater than 1320 °C is able to densify the composites to densities better than 95% T.D. (theoretical density).

CA_6 ($CaO*6Al_2O_3$) is a high temperature phase with an hexagonal structure. The phase has been found at the grain boundaries of 96% Al_2O_3 by Powell-Dogan and Heuer [5]. They reported that CA_6 grew to a plate morphology from the glass phase of SiO_2/MgO/CaO with a strong preferred orientation on α-Al_2O_3 grains. No formation mechanism nor the use of CA_6 as a reinforcing phase are reported in literature.

Lutz and Claussen [6, 7] used porous ZrO_2 agglomerates in a dense matrix to induce compressive zones in a tetragonal zirconia polycrystalline (TZP) matrix. The toughness and strength of the duplex structure have a reverse behavior during thermal quenching, and show an improvement in thermal shock behavior of the TZP ceramics. The present study has selected CA_6/Al_2O_3 composites as the subject, and prepared the composites with two different duplex structures. In the previous study [4], two processing routes were used, either from a hydration and colloidal process of CA particles mixed with Al_2O_3, the other used a dry powder mixture. This report will concentrate on the effects of the CA additive during sintering stages, so as to control the microstructural states of newly grown CA_6 platelets in a dense Al_2O_3 matrix. Also, the thermal shock resistance and the toughening by the duplex structures will be investigated. Possible mechanisms will be reported.

Experimental

Materials

99.7% pure Al_2O_3 powder (A-16SG, Alcoa, PA, USA) and 98% pure CaO powder (with 2% MgO, 150 ppm Fe_2O_3, Nacalai Tesque, Japan) were used as the precursor of CA. Two dispersants, PMAA-N (ammonia salt of polymethyl acrylic acid, R. T. Vanderbilt Co., Morwalk, CT, USA) and semicarbazide hydrochloride (S-HCl Hanawa Chemical Japan), were used for dispersion of the Al_2O_3 suspensions. One deflocculating agent, acetic acid (Showa Chemical, Japan) was used to control

*Corresponding author:
Tel : +886-2-23632684
Fax: +886-2-23634562
E-mail: wjwei@ntu.edu.tw

the gelation of CA-Al_2O_3 admixtures to longer than 50 min.

– Synthesis of CA

CaO was calcined at 750 °C for 2 h in order to get rid of $Ca(OH)_2$. Then the precursors, Al_2O_3 and CaO, were mixed in highly purified iso-propanol in a molar ratio of 1.0 : 1.0. The slurry was ground for 4 h with a Y-ZrO_2 grinding media, and dried in the oven at 105 °C for 2 h. The dried mixture was calcined at 650 °C for 4 h, then at 1300 °C for 5 h. The powder was ground to pass a -400 mesh and showed an average particle size of 11.2 μm. The powder was found to be a pure CA phase by XRD.

Sample preparation

– Dry pressing process

1 to 10 mass% CA powder mixed with Al_2O_3 powder in highly purified iso-propanol, ball-milling for 4 h, and drying in the oven. The mixture was pre-calcined at 650 °C for 3 h before die-pressing, then filled in a rectangular die with the dimensions of 4 × 5 × 45 mm^3. The die surface was coated with a thin layer of stearic acid as a die lubricant. A uniaxial pressure of 85 MPa was applied. The sample was designated "DCA_x", of which D is the die-pressing process, x means the amount of CA in the formulation.

– Hydration reaction process

Al_2O_3 powder in a 40 vol% ratio was added in the aqueous solution with 1 mass% PMAA-N. After mixing for 2 h, the dried CA powder was added and mixed for an additional 5 min. The slurry was cast in a polyacrylic mold with 2 × 6 × 8 cm^3 dimensions, and cured at 50 °C until gelation. The sample was designated "HCA_x".

– Sintering

In order to optimize the shrinkage rate during the formation of the CA_6 phase, the sintering schedule was designed as follows: Room temperature to 650 °C at a rate of 5 K/min, heating to 1200 °C at a rate of 20 K/min, then slowly to 1650 °C at a rate of 2 K/min. Then the composites were finally sintered at 1650 °C for 1 h.

– Comparison case

An Al_2O_3 sample prepared by pressure-filtration and sintered at 1500 °C for 1 h was prepared. The sintered sample had 4% porosity which was comparative to the porosity in the sintered HCA_3 and DCA_3 samples.

Characterization

Thermal expansion of pure sintered Al_2O_3 and CA with the dimensions of 25 × 3.0 × 3.0 mm^3 was measured by dilatometry (α-dilatometer, Theta Industries, Inc., USA). The 4-point fracture strength and single-edge-cracking toughness of the composites were made by following the CNS standards [8] and the report by Nisitani and Mori. [9]

Microstructural analysis was performed using SEM (Philips 515, Netherlands), EPMA (electron probe X-ray micro-analysis, JXA-8600SX, JEOL) on the observation of grain morphology and crack propagation, and quantitative analysis of Ca-elemental distribution.

Thermal shock tests were done by the evaluation of strength degradation of quenched samples. These samples had the same dimensions as the 4-point bending test bars. The bars were held in a tube furnace at a specified temperature up to 350 °C for 30 min, then quenched in a water bath at 25 °C. The dependence of the strength on the quenching temperature gave the critical temperature (ΔT_c).

Results and Discussion

Formation of CA_6 platy structure

Two types of CA_6-Al_2O_3 composites were prepared, either designated as HCA_x or DCA_x. The microstructures of HCA_x samples are shown in Fig. 1. Porous regions approximately in spherical with sizes 20-40 μm were observed and the porosities were 4.5% ($HCA_{1.9}$), 5.0% ($HCA_{3.7}$), and 11% ($HCA_{7.3}$). Most of the porous regions (Fig. 2(a)) were associated with an assembly of

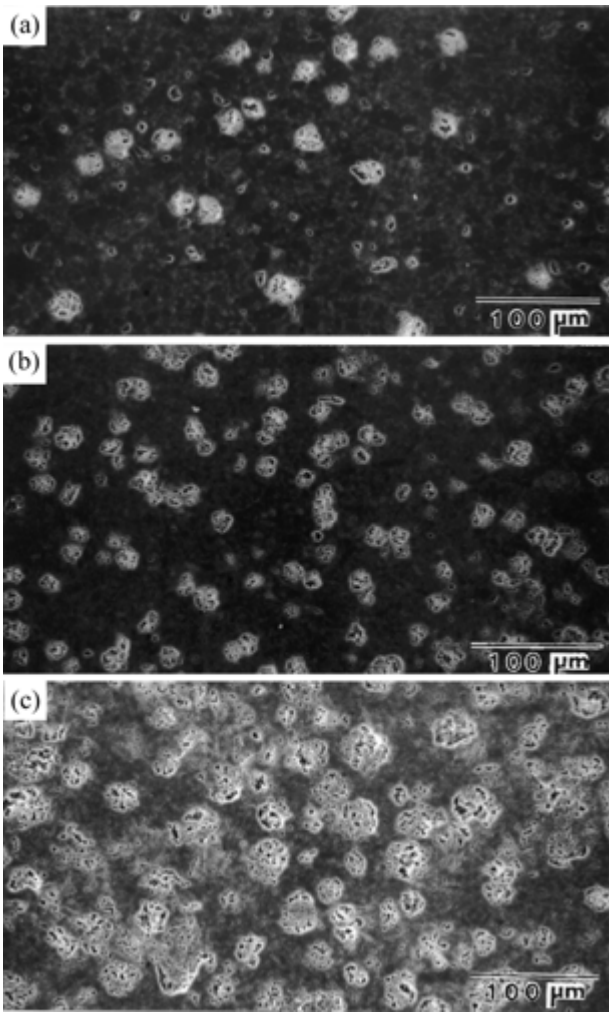

Fig. 1. SEM micrographs of sintered (a) $HCA_{1.9}$, (b) $HCA_{3.7}$ and (c) $HCA_{7.3}$.

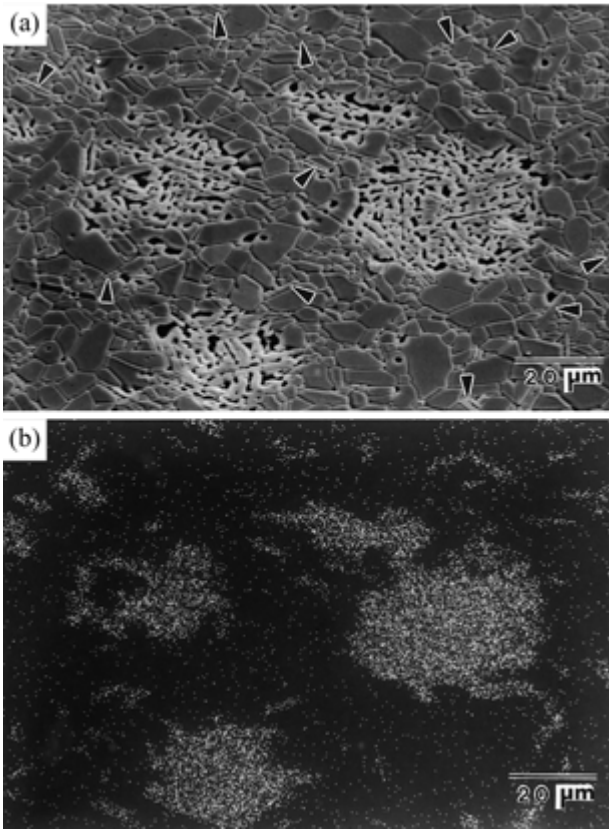

Fig. 2. Micrographs of polished HCA_3 sample (a) imaged with secondary electron signal and (b) X-ray mapping of Ca element. Arrows indicate the CA6 plates embedded in $A1_2O_3$ matrix.

platelet grains, which were identified to be the Ca-rich phase as revealed by X-ray mapping, as shown in Fig. 2(b). In addition, the arrows also indicate in Fig. 2(b) the CA_6 platelets embedded in the $A1_2O_3$ matrix. The Al_2O_3 grains in the matrix have an average grain size of 5.3 μm, the platelets have a length of 10-20 μm and thickness of 0.5-1.0 μm. The eutectic liquid of the CaO-Al_2O_3 system is possibly formed at 1360 °C with a composition close to $C_{12}A_7$. In this study, the addition of CA to Al_2O_3, can form another eutectic liquid at ca. 1600 °C, and help the formation of CA_6 plates. In order to prevent the platelet formation in the early stages of sintering, the sintering was slowly conducted between 1200 to 1600 °C. The matrix can thus be densified and result in the least porosity (4-5%) in the composites.

The volume fraction of the porous CA_6 clusters was estimated, to be close to 13 vol% in HCA_3. The amount of CA_6 clusters was less than the theoretical value of 16%. The difference is due to some CA additive forming discrete platelet CA_6 grains dispersed in the matrix. Several dispersed CA_6 grains were identified from X-ray mapping of Ca element, as pointed in Fig. 2(a). These platelets are formed by the liquid phase reactions of CA-Al_2O_3 or due to the Ca-rich boundaries [2, 3]. The CA particles can be hydrolyzed in the wet-processing stage to a form of C_3AH_6 and $Al(OH)_3$ [10]. A sequence

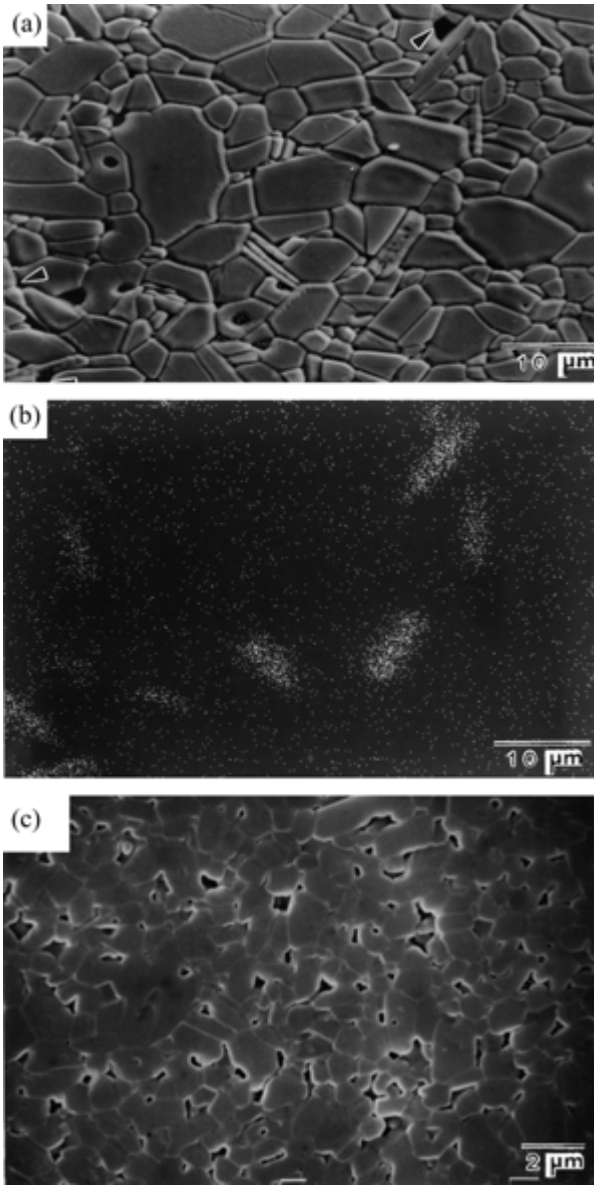

Fig. 3. (a) SEM micrographs and (b) imaged by X-ray mapping of DCA_3 samples (c) sintered Al_2O_3.

of transformation reactions of the hydrates and the reaction with Al_2O_3 took place, finally transforming to CA_6. This resulted in a volume expansion of 2.3 times as big as the original size of CA and the formation of the CA_6 phase.

In comparison, the CA particles were pre-milled and uniformly doped in the Al_2O_3 matrix. Only dispersed CA_6 platelets were found, as shown in Figs. 3(a) and 3(b). The pointed CA_6 grains had an aspect ratio of 3-6. The microstructure was distinct from the pure Al_2O_3 sample (Fig. 3(c)), which appeared with equiaxial Al_2O_3 grains and dispersed porosity.

Crack propagation

SEM micrographs in Fig. 4 illustrate the propagation (along the direction of the arrows) of surface cracks

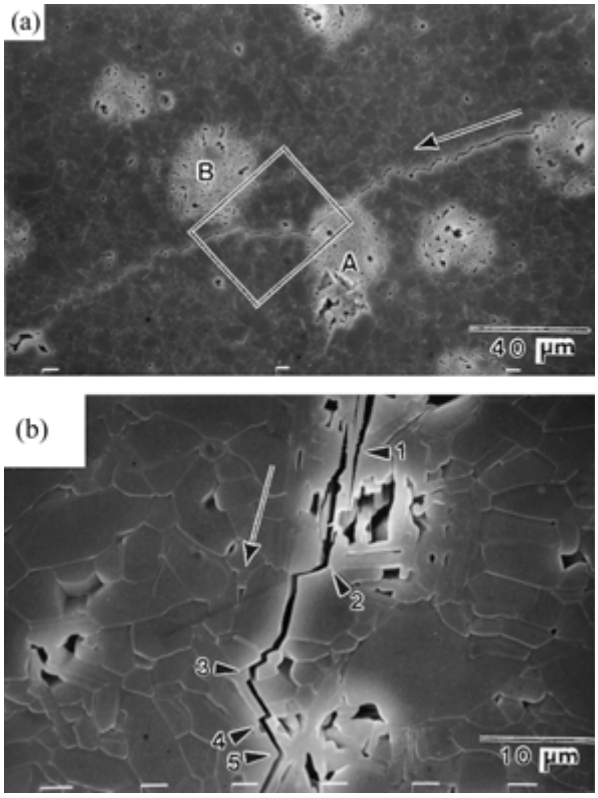

Fig. 4. SEM micrographs illustrating surface crack propagation introduced by an indentation (30 kg load) of (a) HCA_3, (b) DCA_3 composites.

introduced by an indentation with a 30 kg load on the surfaces of HCA_3 and DCA_3 composites. The cracks showed an interesting pattern of interactions with porous CA_6 clusters and separate CA_6 grains. The cracks propagated toward the cluster, then passed the outer interface of the clusters and finally left the cluster in radial direction (Fig. 4(a)). The trajectory of the crack propagation is typical pattern seemly influenced by the residual stresses existing in the matrix and the clusters. These features increase the length of the crack path, resulting in toughening effects. Similar crack deflection and branching were observed in DCA samples, as the features shown in Fig. 4(a). However, the platelets broke, which shows an adverse effect on toughening, as indicated as "4" in Fig. 4(b).

The residual forces come from the differences of thermal expansion coefficients (TEC) between CA_6 and Al_2O_3, of which for pure phases were measured and reported in Fig. 5. The residual stress (P) can be estimated from the equation below [11]:

$$P = \frac{\Delta\alpha\Delta T}{(1+\upsilon_m)/2E_m + (1-2\upsilon_p)/E_p} \quad (1)$$

where $\Delta\alpha$ is the difference of TEC ($\alpha_m - \alpha_p$), ΔT is the quenching temperature range, υ is Poisson's ratio, E is the Young's modulus, and R is the radius of a particular phase (the cluster in this study). If the composites cool from 1400 °C to room temperature, a linear difference

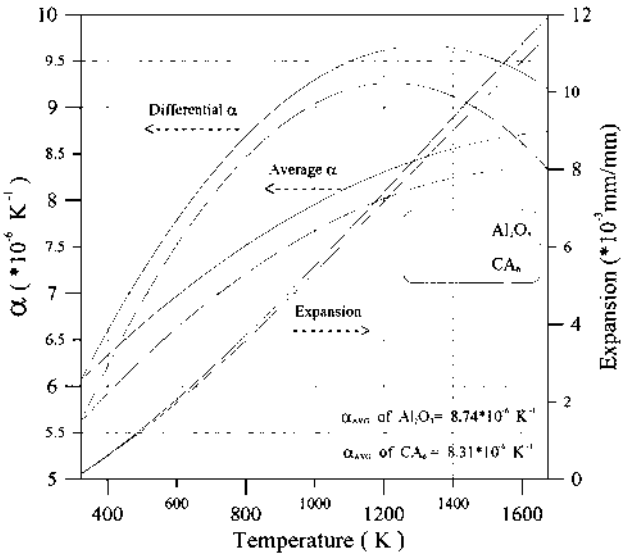

Fig. 5. Linear expansion (mm/mm) and coefficient of expansion coefficient (K^{-1}) of calcium aluminate with CA_6 composition and pure Al_2O_3.

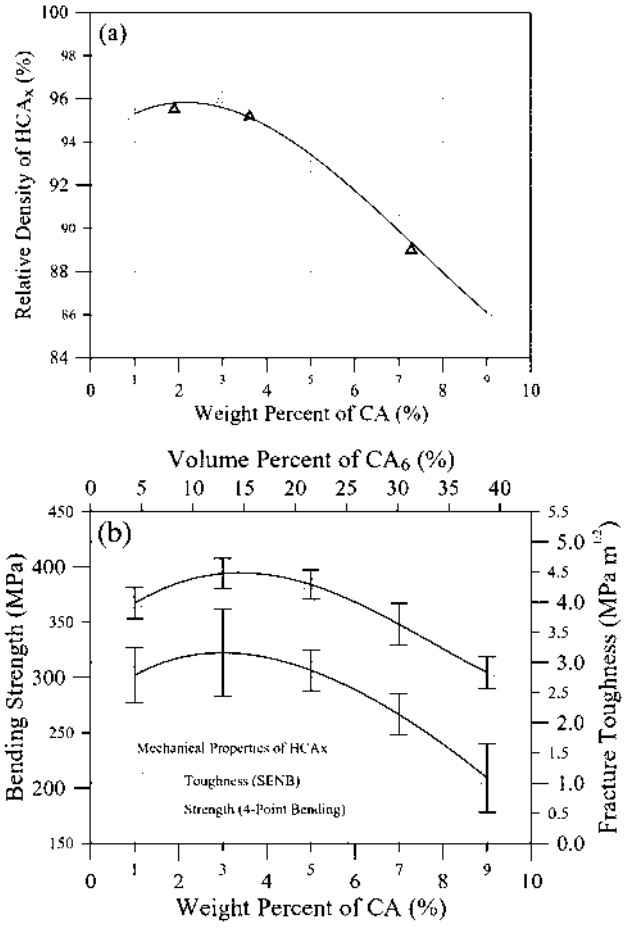

Fig. 6. (a) Relative density and (b) mechanical properties of sintered HCA_x, Note that HCA_3 has the maximum toughness.

of 0.51×10^{-3} is expected (Fig. 5). Also, the Young's modulus of pure CA_6 and Al_2O_3 are 134 GPa and 380

GPa, respectively. If we take 0.25 as the Poisson's ratio for both phases, the calculated residual stress is 93 MPa. A cluster of platelets will have a compressive stress inside with a tangential tensile stress in the matrix. Therefore, the crack can be attracted and deflected by the clusters, and improve the toughness by the duplex structure.

Mechanical Properties at Room Temperature

Figure 6(a) gives the sintered density of HCA_x samples as a function of CA content. The resulting volume% of CA_6 platelets, which was measured from SEM micrographs, is also shown on the axis. The density results showed that the highest density (96% T.D. in Table 1) and strength could be achieved by 3 mass% CA addition, which contained CA_6 clusters of about 13 vol%. A similar trend of the toughness with the maximum value (4.47 $MPam^{0.5}$) of the CA_3 composition is observed in Fig. 6(b). The connection of two clusters was hardly observed in the HCA_3 sample, but occasionally found in the HCA_5, which had 22 vol% of the clusters. Therefore, the strength and toughness of HCA_5 apparently decreased.

Table 1. Summary of mechanical properties of sintered HCA_x, DCA_3 composites and compared to pure Al_2O_3

	A1500	HCA_3	HCA_{10}	DCA_3
Bulk Density (g/cm^3)	3.79	3.81	3.39	–
Relative Density (%)	96	96	86.4	98
R.T. Strength (MPa)	350	310	185	420
ΔT_c (°C)	200	250	260	225
Retain Strength (MPa)	65	105	65	125
Toughness (MPa $m^{1/2}$)	3.80	4.47	–	4.4

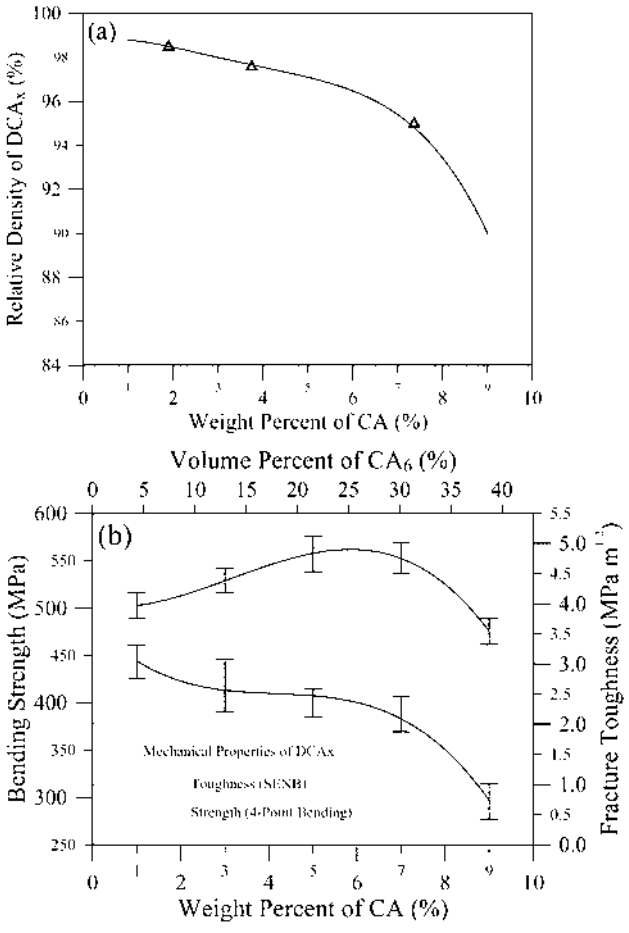

Fig. 7. (a) Relative density and (b) mechanical properties of sintered DCA_x. Note that DCA_5 has the maximum toughness.

The densification results (Fig. 7) of DCA_x was different from HCA_x. The relative density monotonically decreased from 98.5% to 96% T.D., and then dramatically reduced as the CA content was more than 7 mass%. The residual porosity is due to the sintering retardation contributed partially by the formation of CA_6 platelets and also from insufficient green density. The trend of the strength of DCA_x was found to be similar to that of the density. However, the toughness gained a 25% improvement as 5-7% of CA was added, in which 22-30 vol% of CA_6 phase resulted (Fig. 7(b)). The crack deflection (Fig. 4(b)) has reached a maximum toughening effect with 22-30 vol% CA_6 platelets, and slightly reduced strength (10%). If the volume fraction of the CA_6 is greater than 30%, the resulting porosity is more than 10% which greatly reduces the surface fracture energy, and is not a benefit to the toughness.

Thermal Shock Behavior

Three typical test results of the residual strength of the composites are shown in Fig. 8. The detailed properties of all samples, including DCA_3, HCA_3, and A1500 are summarized in Table 1. The critical quenching temperature (ΔT) improved slightly from 200 °C (A1500) to 250 °C (HCA_3) by the CA addition. The best residual strength (σ_r) after shocking was 125 MPa for DCA_3, then the HCA_3 with 105 MPa. The A1500 shows the lowest σ_r (65 MPa). The cracking pattern of HAC_x was similar to that in Fig. 4(a). No debris was found for HCA_x samples.

A residual stress ratio (σ_r/σ_o) was proposed [8] to be linear increase as the parameter (R'''') of thermal shock damage resistance [12, 13]. This is

$$\frac{\sigma_r}{\sigma_o} \propto R'''' \left(= \frac{\gamma E_o}{\sigma_o^2}\right) \tag{2}$$

where E_o is the elastic modulus. The calculated ratio of the surface fracture energies (γ) of A1500, DCA_3, HCA_3 is 1.0 : 2.5 : 1.5. If three parameters, γ, E_o, and σ_o, are considered for the evaluation of R'''', the ratio is 1.0 : 2.0 : 1.6 which is consistent with the test results in Table 1.

Conclusions

The addition of CA particles to an Al_2O_3 matrix has given two different duplex structures, one appeared

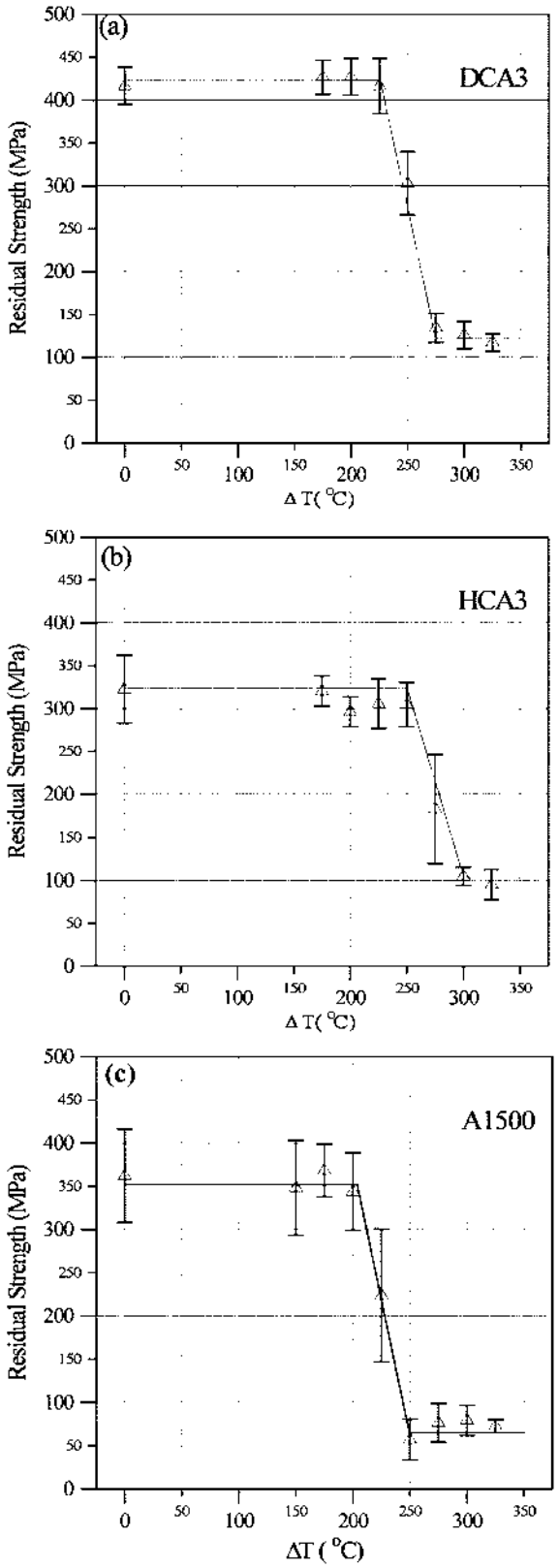

Fig. 8. Residual strength of different samples as a function of quenching temperature. (a) DCA_3, (b) HCA_3, (c) A1500.

with porous clusters filled with CA_6 platelets, the other showed a uniform distribution of the platelets. The density of the composites can be better than 95% which is associated with improved toughness and thermal shock resistance, but a slight sacrifice (<10%) of the fracture strength.

The fracture mode in the dense Al_2O_3 sample was mainly by inter-granular fracture. However, this changed to crack deflection and branching as the CA_6 platelets and clusters are formed in the duplex microstructure. The improvement in the surface fracture energy of the composites was also contributed to an increase of the residual strength and critical quenching temperature. The control of platelet grains in the dense and fragile matrix increases the fracture toughness to some degree.

Acknowledgement

The funding given by National Science Council (NSC84-2216-E-002-034 & NSC85-2216-E-002-031) in Taiwan is appreciated.

Reference

1. R.F. Cook and A.G. Schrott, J. Am. Ceram. Soc. 71[1] (1988) 50-58.
2. S.I. Bae and S. Baik, J. Am. Ceram. Soc. 76[4] (1993) 1065-1067.
3. H. Song and R.L. Coble, J. Am. Ceram. Soc. 73[7] (1990) 2077-2085.
4. W.J. Wei, S.D. Tze, and H.C. Liaw, "Calcium aluminate composites with controlled duplex structures: I. Hydration reaction and densification", (submitted) J. Ceram. Proc. Res.
5. C.A. Powell-Dogan and A.H. Heuer, J. Am. Ceram. Soc. 73[12] (1990) 3670-3691.
6. H.E. Lutz and N. Claussen, J. Europ. Ceram. Soc. 7[4] (1991) 209-226.
7. H.E. Lutz and N. Claussen, J. Am. Ceram. Soc. 74[4] (1991) 11-18.
8. CNS 12701, *Standard tests for the fracture strength of fine ceramics.*
9. H. Nishitani and K. Mori, Tech. Reports of the Kyushu Univ., 58[5] (1985) p. 751.
10. K. Fujii, W. Kondo, and H. Ueno, J. Am. Ceram. Soc. 69[4] (1986) 361-364.
11. R.W. Davidge, *Mechanical Behavior of Ceramics*, Cambridge University, London (1979).
12. J. Nakayama, *Fracture Mechanics of Ceramics*, Vol. 2 p. 759-778, ed. By R.C. Bradt, D.P.H. Hasselman, F. F. Lange, Plenum Press, New York (1974).
13. D.P.H. Hasselman, (Mat. Sci. Res. Vol 5), ed. By W. W. Kriegal and H. Palmor III, Plenum Press, NY (1971).